kiewicz and F. Traganos, in *Genetic Expression in the Cell Cycle*, G. M. Padilla and K. S. McCarty, Sr., Eds. (Academic Press, New York, 1982), p. 103.
5. Z. Darzynkiewicz, T. Sharpless, L. Staiano-Coico, M. R. Melamed, *Proc. Natl. Acad. Sci. U.S.A.* **77**, 6696 (1980); Z. Darzynkiewicz, H. A. Crissman, F. Traganos, J. Steinkamp, *J. Cell Physiol.* **113**, 465 (1982).
6. Effects of dye concentrations, staining time, temperature, and *p*H were determined for three-color staining and analysis of DNA, RNA, and protein in ethanol-fixed CHO cells with the dyes Hoechst 33342, pyronin Y (PY), and fluorescein isothiocyanate (FITC), respectively. Results were used to assess optimum conditions for cell staining. Cycling and noncycling populations of CHO cells were harvested from suspension cultures by centrifugation. The culture medium was aspirated and the cells were fixed in 70 percent cold ethanol for at least 12 hours and then centrifuged. The ethanol was removed and the cells were resuspended in phosphate-buffered saline (PBS; *p*H 7.4) containing Hoechst 33342 (0.5 μg/ml) and FITC (0.1 μg/ml) and stained for at least 30 minutes at room temperature. The staining tubes were then chilled on ice for at least 5 minutes and an equal volume of cold PBS staining solution containing Hoechst 33342 (0.5 μg/ml), FITC (0.1 μg/ml), PY (2.0 μg/ml) was added to the suspension of stained cells. After 5 minutes of staining on ice cells were analyzed in the dye solution in an ice bath. Final cell concentration was maintained at approximately 7.5×10^5 cells per milliliter for analysis in the three-laser system (*9*).
7. D. Arndt-Jovin and T. M. Jovin, *J. Histochem. Cytochem.* **25**, 589 (1977).
8. J. Brachet, *C. R. Soc. Biol.* **133**, 88 (1940); H. J. Tanke, I. A. B. Nieuwenhuis, G. J. M. Koper, J. C. M. Slats, J. S. Ploem, *Cytometry* **1**, 313 (1981); H. M. Shapiro, *ibid.* **2**, 143 (1981); A. Pollack *et al.*, *ibid.* **3**, 38 (1982).
9. J. A. Steinkamp, C. C. Stewart, H. A. Crissman, *Cytometry* **2**, 226 (1982).
10. J. A. Steinkamp and R. D. Hiebert, *ibid.* **2**, 232 (1982).
11. G. C. Salzman, S. F. Wilkins, J. A. Whitfill, *ibid.* **1**, 325 (1981).
12. Chinese hamster cells (line CHO, originally obtained from T. T. Puck) were maintained in exponential growth phase in suspension culture free of mycoplasma contamination in Ham's F-10 medium supplemented with heat-inactivated newborn calf serum (15 percent), penicillin (100 U/ml), and streptomycin (100 μg/ml). CHO cells were synchronized in the G_1 phase by continuous growth for 30 hours in isoleucine-free F-10 medium containing thrice-dialyzed newborn calf serum (15 percent).
13. R. A. Tobey, *Methods Cell Biol.* **6**, 67 (1973).
14. T. Lindmo, *Cell Tissue Kinet.* **15**, 197 (1982).
15. R. Baserga, *Exp. Cell Res.* **151**, 1 (1984).
16. H. A. Crissman, Z. Darzynkiewicz, R. A. Tobey, J. A. Steinkamp, *J. Cell Biol.*, in press.
17. R. Baserga, *J. Cell Physiol.* **95**, 3777 (1978); L. H. Augenlicht and R. Baserga, *ibid.* **89**, 255 (1974).
18. This work was performed under the auspices of the Los Alamos National Flow Cytometry and Sorting Research Resource funded by the Division of Research Resources of NIH (grant P41-RR01315-02), the Department of Energy, and PHS grants 1R0CA23296 and CA 28704.

13 November 1984; 19 December 1984

Angiogenesis Induced by Degradation Products of Hyaluronic Acid

Abstract. *Partial degradation products of sodium hyaluronate produced by the action of testicular hyaluronidase induced an angiogenic response (formation of new blood vessels) on the chick chlorioallantoic membrane. Neither macromolecular hyaluronate nor exhaustively digested material had any angiogenic potential. Fractionation of the digestion products established that the activity was restricted to hyaluronate fragments between 4 and 25 disaccharides in length.*

Hyaluronic acid has been implicated in cell-cell interaction, cell-matrix adhesion, cell motility, and the ordering of the extracellular matrix (*1, 2*). In many developing or remodeling tissues a hyaluronate-rich stroma accompanies cell migration (*1*). Subsequent differentiation and vascular ingrowth are associated with an increase in tissue hyaluronidase activity and a decrease in hyaluronic acid concentration (*3*). Hyaluronate inhibits vascularization of chick embryo limb buds (*4*) and delays or reduces development of granulation tissue and newly formed capillaries around subcutaneous implants (*5*). In this report we describe a further regulatory role for certain products of hyaluronate degradation.

Preparations of both human umbilical (Miles Scientific 36-242-1; Sigma H1751) and bovine vitreous (Sigma H7630) hyaluronic acid were used to minimize the possibility of artifacts produced by contaminating species. Because the major contaminants in such preparations are normally chondroitin 4- and 6-sulfate, a mixed preparation of these (Sigma C3219) was also tested. Each glycosaminoglycan preparation was subjected to enzymatic digestion. Testicular hyaluronidase (Miles Scientific 32-042-1) digests were carried out in 0.1*M* acetate buffer and 0.15*M* NaCl (*p*H 5.4) at an enzyme-to-substrate ratio of 1 to 2 by weight (125 to 250 turbidity-reducing units per milligram of substrate). These were incubated at 37°C for the periods indicated in Table 1, and the reaction was stopped by inactivating the enzyme at 100°C for 5 minutes. The digests were then centrifuged at 2000*g* for 10 minutes, filtered through a glass fiber filter (pore size, 1 μm), and freeze-dried.

We determined angiogenic activity by the chick chorioallantoic membrane (CAM) assay (Fig. 1) (*6*). Hyaluronic acid preparations digested with testicular hyaluronidase for 1 to 10 hours consistently gave a significantly higher proportion of positive responses than undigested control preparations ($P < 0.0003$, χ^2 test). However, 24-hour digests showed largely negative responses and did not differ significantly from the controls. CAM assays with hyaluronic acid and heat-denatured hyaluronidase were also negative. Commercial preparations of hyaluronidase have been reported to be contaminated with a vascular permeability factor (*7*). However, the negative results with denatured hyaluronidase, undigested hyaluronic acid, and the 24-hour digest eliminate this as a major factor in the angiogenic response observed. The possibility that chondroitin sulfate contaminants caused the angiogenic activity is not supported by the results (Table 1).

To further test the hypothesis that the angiogenic activity was due to hyaluronate fragments, we incubated 16 mg of the angiogenic hyaluronate digest for 16 hours with 1000 U of streptomyces hyaluronidase (Sigma H1136) at *p*H 5.0 and 60°C. The reaction was stopped by adding cold trichloroacetic acid, the digest was centrifuged (2000*g* for 30 minutes at 4°C), and the supernatant was exhaustively dialyzed against distilled water and freeze-dried. Hyaluronate digest was also carried through the same procedure without the hyaluronidase. The latter preparation was still angiogenic in the CAM assay, but the streptomyces hyaluronidase digest was not. Since streptomyces hyaluronidase is specific for hyaluronic acid, this is further evidence that the angiogenic component of the original digests is derived from hyaluronate.

An exhaustive digest (24 hours) of hyaluronate with testicular or streptomyces hyaluronidase yields essentially a mixture of tetra- and hexasaccharides.

Table 1. Angiogenic activity of hyaluronidase digests. Numbers in parentheses give the number of preparations tested.

Material tested	Number of eggs showing positive angiogenesis/total number of eggs*			
	No digestion	1 to 2 hours	4 to 10 hours	>24 hours
Hyaluronic acid	3/23 (9)	28/45 (18)	41/45 (18)	4/19 (7)
Chondroitin 4- and 6-sulfate	1/8 (5)	3/24 (10)	2/16 (7)	0/10 (5)

*Control results: heat-inactivated hyaluronidase, 4/18 (7); hyaluronidase buffer, 1/13 (6); native hyaluronate, 3/25 (10); native chondroitin 4- and 6-sulfate, 4/19 (7).

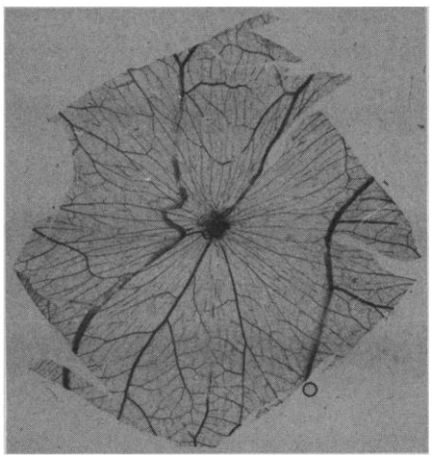

Fig. 1. Excised chick CAM showing a positive angiogenic response to hyaluronic acid fragments. Each sample was tested with three separate eggs. A freeze-dried powder was placed on a discrete area of the CAM of a 10-day chick embryo and the CAM was examined 3 and 4 days later. The CAM was assessed under blind conditions as showing either a "spoked-wheel" pattern of vessels radiating from the point of sample application (positive response) or a lack of any detectable change or merely a slight distortion of the surrounding vessels (negative response) (*6*).

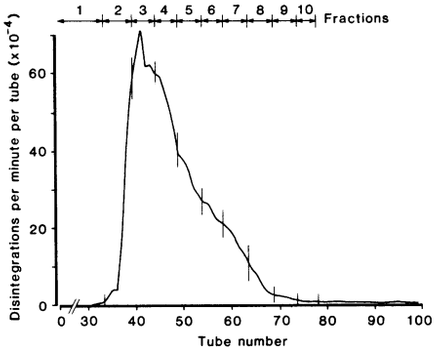

Fig. 2. Elution profile of a polydisperse preparation of tritiated hyaluronate oligosaccharides (4×10^8 count/min) prepared by testicular hyaluronidase digestion of fibroblast hyaluronic acid (*9*, *10*). The sample (10 ml) was dissolved in 4*M* guanidine hydrochloride and 50 m*M* phosphate (*p*H 6.5) and applied to a column of Sephacryl S300 (90 by 2.5 cm) equilibrated in the same buffer. The column was eluted at 10 ml hour and 100 4.8-ml portions were collected. A 100-μl aliquot of each portion was taken for scintillation counting. Fractions 2 to 10 were obtained by combining tubes 32 to 37, 38 to 42, 43 to 47, 48 to 52, 53 to 57, 58 to 62, 63 to 67, 68 to 72, and 73 to 77, respectively. Each fraction was dialyzed, freeze-dried, and subjected to PAGE.

Table 2. Angiogenic activity of hyaluronate fragments from the Sephacryl S300 fractions. Unlabeled hyaluronate (8 mg) was digested with testicular hyaluronidase for 1, 2, 4, or 8 hours. The reaction was stopped by heating (100°C for 5 minutes) and the resultant precipitate removed by centrifugation (1000*g* for 30 minutes). Trichloroacetic acid was added to the supernatant to give a final concentration of 20 percent (weight to volume) and the precipitate was removed by centrifugation, neutralized with Na_2CO_3, dialyzed, and freeze-dried. All the fractions were pooled and the whole was fractionated on a Sephacryl S300 column. The results are for three separate preparations, and both vitreous and umbilical hyaluronate were tested on CAM's.

Pooled Sephacryl S300 fractions	Number of positive responses/ number of tests	Oligosaccharide size range (disaccharide units)
2	1/9	>100
3	0/5	20 to >100
4	1/5	21 to >100
5	1/5	21 to 80
6	1/6	20 to 65
7	3/6	13 to 45
8	4/8	8 to 23
9	2/5	5 to 12
10	7/8	3 to 5

Because such digests are not angiogenic, the fragments with angiogenic activity must be more than three disaccharides long. A more precise estimate of the size of the angiogenic fragments was obtained with (i) a Sephacryl S300 column that had been calibrated with a polydisperse sample of tritiated hyaluronate fragments and (ii) polyacrylamide gel electrophoresis (PAGE) (Figs. 2 and 3) (*10*). Successive timed digests of unlabeled hyaluronic acid were made with testicular hyaluronidase and pooled to give a polydisperse population of hyaluronate fragments, which was then fractionated on the S300 column. The fractions were dialyzed, freeze-dried, and assayed for their ability to induce angiogenesis (Table 2).

Hyaluronic acid oligosaccharides in fractions 7 to 10 induced significantly more angiogenic responses in the CAM assay than fractions 2 to 6 ($P < 0.0008$, χ^2 test). It therefore appears that degradation products consisting of 3 to 45 disaccharides are angiogenic. However, the electrophoretic patterns of fractions 6 (negative fragments) and 7 (positive fragments) overlap considerably. If the major species in fraction 6 are not angiogenic, then the upper size limit of angiogenic oligosaccharides is approximately 25 disaccharides. Therefore the active hyaluronate fragments seem to contain 4 to 25 disaccharides.

For the initial screening of angiogenic activity, we placed up to 0.5 mg of the fraction on the CAM. To determine the minimum amount of fragments required to induce angiogenesis, fractions 7 to 10 were pooled and dissolved in 1 percent bovine serum albumin, and 25-μl aliquots containing 0.5 to 500 μg of hyaluronate fragments were placed on sterile cover slips for the CAM assay. We found that 5 μg or more of the oligosaccharide produced a positive angiogenic response, whereas 1 μg or less proved negative. Furthermore, hyaluronate fragments outside the size range 4 to 25 disaccharides, chondroitin 4- and 6-sulfate, and degraded chondroitin sulfates

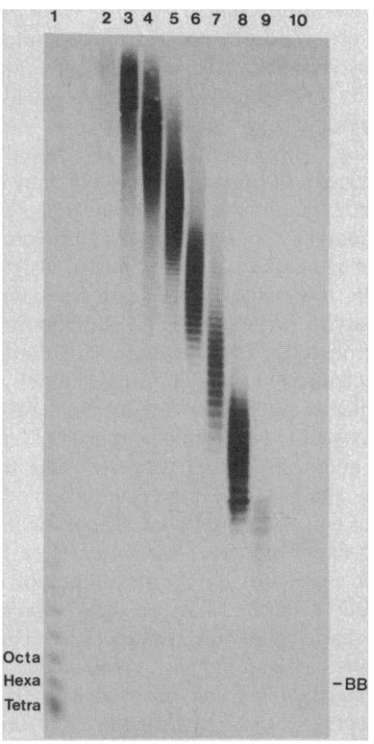

Fig. 3. Polyacrylamide gel electrophoresis of radioactive hyaluronate oligosaccharides that had been separated into fractions of broad molecular size ranges by gel filtration of Sephacryl S300 (Fig. 2) (*9*). A 10-μl tritiated sample ($\sim 3.5 \times 10^4$ count/min) was applied to each track of a 40 cm by 20 cm by 1 mm 15 percent polyacrylamide slab gel. Electrophoresis was performed at 600 V and 35 mA for approximately 4 hours with tris-glycine buffer (*p*H 8.9) and the dyes phenol red and bromophenol blue) (BB). The gel was fixed in diphenyloxazole (20 percent, weight to volume) in glacial acetic acid and radioactive bands were detected by fluorography. Track I, reference labeled hyaluronate oligosaccharides (size determined with BioGel P6); track 2, S300 fraction 2; track 3, fraction 3; track 4, fraction 4; track 5, fraction 5; track 6, fraction 6; track 7, fraction 7; track 8, fraction 8; track 9, fraction 9; and track 10, fraction 10. Material exhaustively digested with hyaluronidase was not angiogenic and gave two main bands and one minor band corresponding to those labeled tetra-, hexa-, and octasaccharide in track 1 (size determined with BioGel P6). Track 10 is not visible on the photographic plate; however, bands going down to tetrasaccharide can be seen when viewed by indirect light on the x-ray film.

were not angiogenic at 100 times this concentration.

These observations suggest that the degradation of hyaluronic acid in developing or remodeling tissues may not only remove the antiangiogenic activity of the native hyaluronate but also produce fragments that are angiogenic. The mode of action of the hyaluronate degradation products has yet to be determined. However, hyaluronic acid is known to bind to and modulate the interaction of fibronectin with collagen (*12*), aggregate proteoglycans (*13*), and self-associate to a considerable degree (*14*). Hyaluronate oligosaccharides (similar in size to the angiogenic fragments) inhibit many of these interactions (*11, 12, 14*). Recently several proteins were isolated from the extracellular matrix and found to be able to bind to hyaluronate; they appear to be involved in structuring the extracellular matrix. It is reasonable to assume that hyaluronate fragments would also interfere with their function. Thus the stimulation of angiogenesis may be due to a "loosening" or disorganizing effect on the extracellular matrix and a weakening of cell-cell and cell-matrix interactions.

Electron microscopy has shown significantly more small vessels in ischemic areas of infarcted myocardium from animals treated with high doses of hyaluronidase than in such tissue from untreated animals (*15*). Furthermore, hyaluronate has been implicated in the invasive growth of tumors, which have been shown to produce hyaluronidase (*16*). In several disease conditions (rheumatoid arthritis, osteoarthritis, and diabetic retinopathy), vascularization occurs close to a hyaluronate-rich fluid. In rheumatoid arthritis a decrease in the molecular weight of joint fluid hyaluronate may be due in part to the action of hyaluronidase or oxygen radicals (*17*).

Although numerous angiogenic factors have been detected (*18*), none has been adequately characterized. We have now identified a new angiogenic factor and determined its size distribution. The ubiquitous presence of hyaluronate in tissues suggests that the native and degraded forms are important in the control of normal and pathological neovascularization. An understanding of the mode of action of these angiogenic fragments may enable us to modulate the angiogenic process.

D. C. West
I. N. Hampson
F. Arnold
S. Kumar

Christie Hospital,
Manchester M2O 9BX, England

References and Notes

1. B. P. Toole, in *Cell Biology of the Extracellular Matrix*, E. D. Hay, Ed. (Plenum, New York, 1981), pp. 259–294; L. A. Culp, *Curr. Top. Membr. Transp.* **11**, 327 (1978).
2. H. Muir, *Biochem. Soc. Trans.* **11**, 613 (1984); E. Turley and D. Moore, *Biochem. Biophys. Res. Commun.* **121**, 808 (1984).
3. B. P. Toole, in *Neuronal Recognition*, S. H. Baronades, Ed. (Plenum, New York, 1976), pp. 275–329; E. Belsky and B. P. Toole, *Cell Differ.* **12**, 61 (1983).
4. R. N. Feinberg and D. C. Beebe, *Science* **220**, 1177 (1983).
5. E. A. Balazs and Z. Darzykiewicz, in *Biology of Fibroblast*, E. Kulonen and J. Pikkarainen, Eds. (Academic Press, New York, 1973), pp. 237–252; N. Rydell and E. A. Balazs, *Clin. Orthop.* **80**, 25 (1971).
6. S. Kumar *et al.*, *Lancet* **1984-II**, 364 (1984).
7. J. C. Houck and C. M. Chang, *Inflammation* **3**, 447 (1979).
8. T. Yamagata *et al.*, *J. Biol. Chem.* **243**, 1523 (1968).
9. I. N. Hampson and J. T. Gallagher, *Biochem. J.* **221**, 697 (1984).
10. J. T. Gallagher *et al.*, *ibid.* **215**, 107 (1983).
11. S. Eriksson *et al.*, *Exp. Cell. Res.* **144**, 223 (1983).
12. K. M. Yamada, in *Cell Biology of the Extracellular Matrix*, E. D. Hay, Ed. (Plenum, New York, 1981), pp. 9–114; H. Hormann and V. Jelinic, *Hoppe-Seyler's Z. Physiol. Chem.* **362**, 87 (1971).
13. V. C. Hascall and Heinegard, *J. Biol. Chem.* **249**, 4242 (1974).
14. E. R. Morris, D. A. Rees, E. J. Welsh, *J. Mol. Biol.* **138**, 383 (1980).
15. R. A. Klorier, M. C. Fishbain, D. Maclean, *Am. J. Cardiol.* **40**, 43 (1977).
16. B. P. Toole, B. Chitra, J. Gross, *Proc. Natl. Acad. Sci. U.S.A.* **76**, 6299 (1979).
17. J. C. Caygill, in *Carbohydrate Metabolism and Its Disorders*, F. Dickens, P. J. Randle, W. J. Whelan, Eds. (Academic Press, New York, 1968), vol. 1, pp. 223–263; E. R. Berman and M. Voaden, in *Biochemistry of the Eye*, C. N. Graymore, Ed. (Academic Press, New York, 1970), pp. 373–471; H. Furthmayr and R. Timpl, *Int. Rev. Connect. Tissue Res.* **7**, 61 (1976).
18. A Fenselau, Ed., *Oncology Overview* (National Cancer Institute, Bethesda, Md., 1983).
19. The technical help of J. Heslop and N. Evans is gratefully acknowledged. We also thank R. Stoddart and D. Harnden for their valuable advice and criticism. D.C.W. is supported by the Medical Research Council. S.K. is in receipt of grants from the Wellcome Foundation and British Heart Foundation.

13 September 1984; accepted 25 March 1985

Dragonfly Flight: Novel Uses of Unsteady Separated Flows

Abstract. *Studies of insect flight have revealed novel mechanisms of production of aerodynamic lift. In the present study, large lift forces were measured during flight episodes elicited from dragonflies tethered to a force balance. Simultaneously, stroboscopic photographs provided stop-action views of wing motion and the flow-field structure surrounding the insect. Wing kinematics were correlated with both instantaneous lift generation and vortex-dominated flow fields. The large lift forces appear to be produced by unsteady flow-wing interactions. This successful utilization of unsteady separated flows by insects may signal the existence of a whole new class of fluid dynamic uses that remain to be explored.*

Many insect species exhibit flight behaviors not readily explained by conventional steady-state aerodynamics (*1, 2*). Using high-speed photographic records of hovering chalcid wasps, Weis-Fogh (*2*) observed a wing upstroke completed by a dorsal clap and a downstroke initiated by a flinging apart of the wing leading edges. These so-called "clap" and "fling" movements were purported to induce both temporally and spatially dependent circulations about the wings that accounted for large unsteady lift forces. The estimated lift values were consistent with the observed hovering behavior. Analytic evaluations (*3*) corroborated the postulated underlying unsteady fluid mechanics. Using physical models to simulate the Weis-Fogh mechanism, Maxworthy (*4*) visualized these unsteady separated flows and suggested that they play a larger role in the production of lift than had been predicted. Theoretical (*5*) and experimental (*6*) analyses have further characterized the influences of unsteady separated flow on the Weis-Fogh mechanism of lift production. These studies indicated that novel unsteady fluid mechanisms can be used by certain insects. Moreover, these unsteady separated flow mechanisms, based on the same wing geometry and kinematics, appear to generate more lift than do steady-state mechanisms.

In this study we correlated dragonfly wing kinematics with lift history and the structure of the surrounding flow field. This insect exhibits a proficient flight capability with relatively simple, fixed-geometry wings. Its major flight modes include stationary hovering or slow hovering in any direction, high-speed upward and forward flight, and gliding flight. Earlier studies (*2, 7*) indicated that, for dragonfly hovering, calculations based on steady-state aerodynamic theory do not produce the lift values necessary to counterbalance the weight of the insect (*8*). In fact, the large geometric attack angles of the wings characteristic of dragonfly hovering may result in a total separation of the boundary layer that precludes the use of steady-state mechanics.

In evaluating the mechanisms of dragonfly flight, physical characteristics were measured, wing kinematics were documented photographically, lift production was correlated with wing motions, and flow was visualized to reveal